Regulation of Skin Collagen Metabolism *In Vitro* Using a Pulsed 660 nm LED Light Source: Clinical Correlation with a Single-Blinded Study

Daniel Barolet[1,2], Charles J. Roberge[3], François A. Auger[3,4], Annie Boucher[1] and Lucie Germain[3,4]

It has been reported that skin aging is associated with a downregulation in collagen synthesis and an elevation in matrix metalloproteinase (MMP) expression. This study investigated the potential of light-emitting diode (LED) treatments with a 660 nm sequentially pulsed illumination formula in the photobiomodulation of these molecules. Histological and biochemical changes were first evaluated in a tissue-engineered Human Reconstructed Skin (HRS) model after 11 sham or LED light treatments. LED effects were then assessed in aged/photoaged individuals in a split-face single-blinded study. Results yielded a mean percent difference between LED-treated and non-LED-treated HRS of 31% in levels of type-1 procollagen and of −18% in MMP-1. No histological changes were observed. Furthermore, profilometry quantification revealed that more than 90% of individuals showed a reduction in rhytid depth and surface roughness, and, via a blinded clinical assessment, that 87% experienced a reduction in the Fitzpatrick wrinkling severity score after 12 LED treatments. No adverse events or downtime were reported. Our study showed that LED therapy reversed collagen downregulation and MMP-1 upregulation. This could explain the improvements in skin appearance observed in LED-treated individuals. These findings suggest that LED at 660 nm is a safe and effective collagen-enhancement strategy.

Journal of Investigative Dermatology (2009) **129,** 2751–2759; doi:10.1038/jid.2009.186; published online 9 July 2009

INTRODUCTION

Skin aging, intrinsic and extrinsic, is associated with morphological changes, including rhytids, furrows, and telangiectasia (Kang *et al.*, 2001; Fisher *et al.*, 2002). It has been reported that collagen synthesis is reduced and interstitial matrix metalloproteinases (MMP-1), the collagenase involved in normal turnover of skin collagen, are upregulated in aged skin (Fligiel *et al.*, 2003; Fisher *et al.*, 2008; Varani *et al.*, 2004). Hence, a possible strategy for treating and preventing clinical manifestations of skin aging is the restoration of collagen deficiency by the induction of new collagen synthesis and reduction of MMP-1.

It has been shown that light-emitting diode (LED) therapy, a nonthermal noninvasive treatment, can trigger natural intracellular photobiochemical reactions (Karu and Kolyakov, 2005; Karu *et al.*, 2005a, b; Hamblin and Demidova, 2006; Barolet, 2008). A number of clinical studies provide evidence of the effectiveness of LED therapy in photorejuvenation using a variety of LED light sources (Weiss *et al.*, 2004; Bhat *et al.*, 2005; Russell *et al.*, 2005; Weiss *et al.*, 2005; Goldberg *et al.*, 2006; Baez and Reilly, 2007; Lee *et al.*, 2007). An improvement in skin appearance in aged/photoaged individuals has been documented after full-face or split-face serial treatments with yellow (590 nm), red (630, 633 nm), or red in combination with infrared (830 nm) light based on profilometry quantification, clinical assessment of digital photographs, and patient reported outcomes. A correlation of clinical effects with further analysis for basic mechanisms was examined in two of these studies. In Weiss *et al.* (2005), after a regimen of eight treatments delivered over 4 weeks with LED 590 nm, staining with anti-collagen I antibodies showed a 28% (range of 10–70%) average increase in density, whereas staining with anti-MMP-1 showed an average reduction of −4% (range of −2 to −40%). In the Lee *et al.* study, participants were randomly divided into four groups treated with either 830 nm alone, 633 nm alone, a combination of 830 and 633 nm, or a sham treatment light, two times a week for 4 weeks. In the treatment groups, a significant increase in the amount of collagen was observed by histological evaluation with standard preparation with hematoxylin and eosin stain. This finding was confirmed by

[1]*RoseLab Skin Optics Laboratory, Montreal, Quebec, Canada;* [2]*Department of Medicine, Dermatology Division, McGill University, Montreal, Quebec, Canada;* [3]*Laboratoire d'Organogénèse Expérimentale (LOEX), Centre de recherche (FRSQ) du CHA de Québec, Centre de recherche du CHA de Québec, Hôpital du Saint-Sacrement du CHA (FRSQ), Quebec, Canada and* [4]*Department of Surgery, Laval University, Quebec, Canada*

Correspondence: Dr Daniel Barolet, RoseLab Skin Optics Laboratory, 3333 Graham Blvd., Suite 206, Montreal, Quebec, CANADA H3R 3L5. E-mail: daniel.barolet@mcgill.ca

Abbreviations: FCS, Fitzpatrick Classification System; HRS, human reconstructed skin; LED, light-emitting diode; MMP-1, matrix metalloproteinase-1

Received 7 January 2009; revised 15 April 2009; accepted 30 April 2009; published online 9 July 2009

the Masson–trichrome stain for collagen. In the immunohistochemical staining results, no significant changes in MMP-1 or MMP-2 were observed between the baseline and 2 weeks posttreatment specimens in all groups. Other models have also been used to investigate LED-based effects. Collagen increase after LED treatment has been documented in fibroblast cultures (McDaniel *et al.*, 2002; Huang *et al.*, 2007), in third-degree burn wound-healing models (Meireles *et al.*, 2008a, b), and in human blister fluids (Barolet *et al.*, 2005). However, concurrent MMP determinations after LED treatment were not assessed in these experiments.

In this study, we opted for an innovative approach involving a stable *in vitro* model replicating a real-life LED clinical application, and then sought to explore clinical correlates of these effects in humans. The 660 nm LED light source delivered in a sequential pulsing mode was used as it is a deep penetrating well-absorbed wavelength that falls into the absorption peaks of cytochrome *c* oxidase, the chromophore thought to be responsible for LED effects (Karu and Kolyakov, 2005; Karu *et al.*, 2005a, b).

A 3-D model of tissue-engineered Human Reconstructed Skin (HRS) (Michel *et al.*, 1999) was used to initially investigate the potential of 660 nm LED in modulating collagen and MMP-1. The HRS model offers a variety of advantages over other *in vitro* and preclinical models. HRS samples are produced exclusively from human fibroblasts and keratinocytes and do not contain any synthetic material. This model emulates skin as a complex tissue composed of two different compartments, the continuously renewing epidermis made up mostly of keratinocytes and the underlying dermal matrix with fibroblasts as its major cellular components. These compartments are tightly interconnected allowing for paracrine mutual interactions, which are essential for epidermal growth, differentiation, and tissue homeostasis. This HRS model represents a unique opportunity to test biological changes after LED treatment over an extended time frame on age- and gender-defined skin, much like a clinical setting. Eleven consecutive LED treatments carried out over 4 weeks were conducted on HRS and compared with the untreated control specimens for type I procollagen and MMP-1 production. The clinical study was then conducted to corroborate the *in vitro* experiment. A group of chronologically aged/photoaged individuals received 12 LED treatments or a sham light control over a 1-month period (split-face study). Clinical improvements were assessed with an *in vivo* 3-D microtopography quantitative measurement (PRIMOS readings) and a qualitative clinical assessment of digital photographs by blinded medical observers. Our results supported the hypothesis that LED treatments could upregulate collagen and downregulate MMP-1 *in vitro*, and thus lead to improvements in skin appearance observed in the LED-treated side in humans.

RESULTS

LED-induced modulations in type I procollagen and MMP-1 production of human reconstructed skin

Type I procollagen and MMP-1 production was assessed in the supernatants of HRS from individuals with aged/photoaged skin

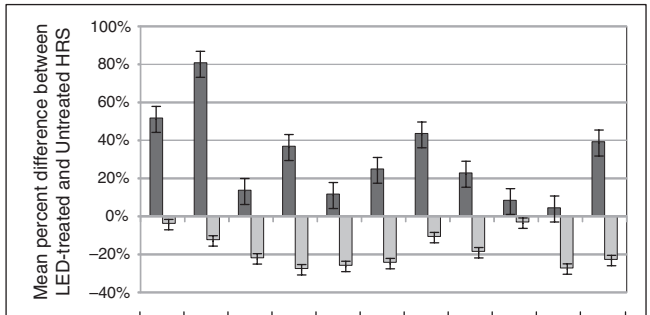

	T1	T2	T3	T4	T5	T6	T7	T8	T9	T10	T11
Cohen's *d* type-1 procollagen	0.64	1.20	0.28	0.59	0.30	0.50	0.56	0.66	0.22	0.09	0.68
Cohen's *d* MMP-1	–0.12	–0.42	–0.75	–1.01	–0.68	–0.45	–0.46	–0.59	–0.08	–0.56	–0.65

Figure 1. Increases in type I procollagen and concurrent reduction in MMP-1 levels in HRS after LED treatment. A cyclic pattern of alternating highs and lows was observed in response to the 11 consecutive treatments (T1–T11) for type 1 procollagen and MMP levels. Values are percent difference ± SEM ($n = 9$) between treated and untreated control HRS samples in mean levels of type I procollagen and MMP-1 assessed in the supernatants after each treatment. Table shows Cohen's *d* for type 1 procollagen and MMP-1 for each time point.

in response to each of the 11 LED treatments (T1–T11) conducted over a 1-month period. An increase in type I procollagen production with a concomitant decrease in MMP-1 levels was observed in the LED-treated samples when compared with that in untreated samples. The latter effects were found to be cyclic, with alternating high and low levels observed in response to consecutive LED treatments The mean percent difference between LED-treated and untreated HRS specimens across repeated treatments was 31% (range of 5–81%) for type I procollagen levels and −18% (range of −3 to −27%) for MMP-1 levels (Figure 1). Cohen's *d* effect size was in the medium-to-large range at the various time points for both type-1 procollagen and MMP-1 measurements, with the exception of T9 ($d \leqslant 0.2$) (see Table below Figure 1).

Histological assessments on HRS

Morphological changes after the last LED treatment were assessed using Masson's trichrome and immunofluorescent staining. Masson staining of reconstructed skin showed no histological difference in the extracellular matrix (same dermal thickness) in LED-treated compared with untreated control samples (data not shown). Typical results from an LED-treated HRS are depicted in Figure 2a (HRS38). Immunofluorescent staining of HRS yielded no difference in the amounts of type I procollagen (same band thickness) between the LED-treated and untreated specimens (data not shown). A representative fluorescent immunostaining pattern after LED treatment for type I procollagen is displayed in Figure 2b. Overall, after LED treatments, the dermal layer exhibited a dense well-organized collagenous connective tissue material, overlaid with a well-stratified epidermis, presenting an intact stratum basale.

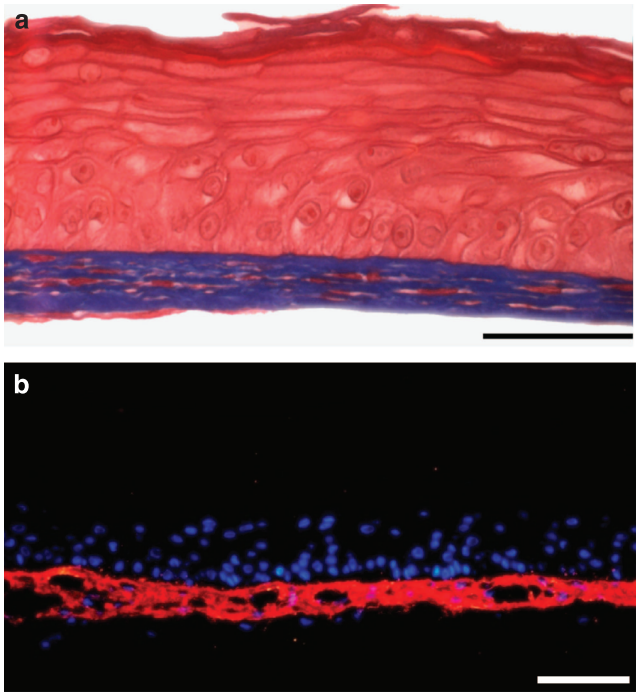

Figure 2. Histological assessments of HRS. (**a**) Masson stain after LED treatment on reconstructed skin (HRS38), underlining the presence of dermal collagen (colored in blue) in the dermal portion. Keratinocytes found in the epidermis and dermal fibroblasts are colored in red. (**b**) Fluorescent immunostaining of HRS42 type I collagen located in the dermal portion (red band pattern) after LED treatment. Nuclei are colored in blue for both keratinocytes (round nuclei) and dermal fibroblasts (elongated nuclei). No morphological changes were observed on HRS after LED treatments. Scale bar indicates 50 μm.

Table 1. Microtopographic profilometry analysis

	Percent improvement post-treatment			Percentage of subjects with improvement	
	LED-treated	Untreated	*P*-value	LED-treated (%)	Untreated (%)
Ra	18.57 ± 2.41	3.73 ± 1.17	<0.0001	97	46
Rz	20.83 ± 2.26	7.43 ± 1.64	<0.0001	94	51

Values are mean ± SEM.

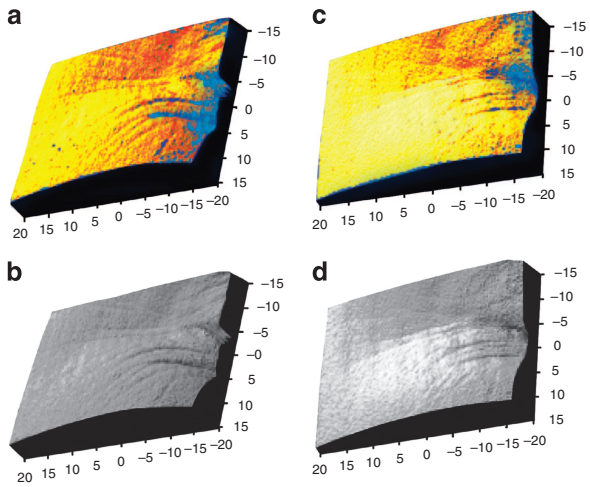

Figure 3. Reduction in rhytids and skin roughness with LED therapy. Photograph depicts color-coded topography images before treatment (**a**) and after LED treatment (**c**). Each color determines a specific depth with darker areas indicating a deeper wrinkle surface. Black and white photographs show skin texture and pore size for the pre-LED (**b**) and post-LED treatment areas (**d**). All photographs are for S2 aged 38 years.

Profilometry quantification of improvements in skin appearance

To assess the potential of 660 nm LED light in improving the appearance of aged/photoaged skin, participants were treated weekly three times for four consecutive weeks (12 treatments) with an LED and sham light contralaterally in a split-face design. Results from a microtopographic profilometry analysis (PRIMOS reading) of rhytid depth and severity (Rz) and reduction in skin roughness (Ra) are presented in Table 1. Analysis of the results showed that the percent improvement after treatment in Rz values was statistically different between the LED-treated and control non-treated sides ($P<0.0001$). LED treatment produced an Rz reduction in 94% of participants, with the highest reduction in rhytids of 51% noted on a female participant aged 46 years (S33). For the non-treated side, Rz reductions were observed in 51% of participants. The results from the LED-treated side also revealed a statistically significant reduction in surface roughness in comparison with the untreated control side ($P<0.0001$), as measured by Ra. Overall, an improvement in skin appearance after LED treatment was observed in 97% of participants, with the highest benefit of 56% observed on a woman aged 57 years (S29). For the untreated side, improvements were observed in 46% of participants. The participant's age was not found to influence the effect of LED treatment on Rz or Ra values. Figure 3 shows PRIMOS phase shift black and white and color-coded microtopography photographs before and after LED therapy of the periorbital area for participant S2.

Skin textural enhancement in aged/photoaged participants

Clinical assessment of digital photographs taken before treatment and after the last treatment were analyzed by three blinded medical observers. According to the observers, an improvement in at least one subtype of the Fitzpatrick Classification System (FCS), used to evaluate the degree of wrinkling (rhytids), was obtained in 85–90% (mean of 87%) of participants after LED treatments. For the untreated side, an improvement was observed in 25–63% of participants (mean of 45%). Observer assessments revealed that the degree of improvements in wrinkling after treatment was mild to moderate. The analysis conducted on severity scores showed that there was a significant difference between the LED-treated and untreated sides for Observers 1 ($P<0.0001$) and 3 ($P=0.001$), but not according to Observer 2 (Table 2). Results were not found to be influenced by the participant's

Table 2. Observers' assessment of improvement in the severity of wrinkles

	Degree of improvement			Percentage of subjects ⩾1 point	
	LED-treated	Untreated	*P*-value	LED-treated (%)	Untreated (%)
Observer 1	1.35 ± 0.11	0.25 ± 0.07	<0.0001	90	25
Observer 2	0.90 ± 0.07	0.70 ± 0.10	NS	85	63
Observer 3	1.03 ± 0.09	0.50 ± 0.09	0.001	85	48

Values are mean ± SEM; NS: non-statistically significant.

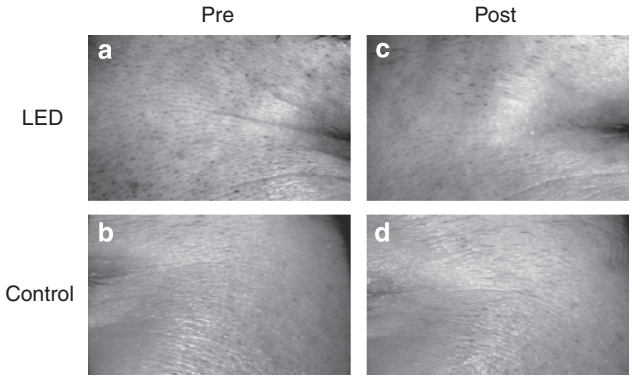

Figure 4. Improvements in skin appearance in aged/photoaged participants with LED treatment. Digital photograph illustrates periorbital areas at pre-treatment (**a**) and posttreatment (**c**) for the LED-treated side, and at pre-treatment (**b**) and posttreatment (**d**) for the non-treated control area. All photographs are for S2 aged 38 years.

age. The internal consistency between the observers' findings was deemed to be acceptable (Cronbach's $\alpha = 0.615$). Clinical results for participant S2 are displayed in Figure 4.

Skin temperature steadiness during LED treatment

It has been reported that a mild increase in temperature (43 vs 37°C) can induce a decrease in type I procollagen secretion (Halper *et al.*, 2005). Papillary dermis temperature was thus monitored in our clinical study throughout LED exposure to ensure that skin temperature was kept normal in order not to hinder photobiochemical reactions associated with collagen metabolism. Monitoring attested that physiological temperature was maintained at the treatment area during the entire procedure. Temperature variations registered by thermocouple probes during LED treatment were stable or never more than 0.5°C (dermo-epidermal junction temperature of 33 ± 0.5°C).

LED therapy safety profile in humans

Adverse reactions were monitored throughout the study. LED therapy was found to be well tolerated by all patients, with no adverse effects or downtime reported during or after LED treatment.

DISCUSSION

This study investigated the potential of 660 nm sequentially pulsed LED treatments in the photoinduction of collagen synthesis and MMP-1 modulation in humans. LED-induced biochemical and histological changes in a 3-D HRS *in vitro* model were first examined. A clinical study was then carried out to assess *in vivo* the clinical correlates of this light treatment on skin texture and appearance of individuals with aged/photoaged skin, in whom collagen synthesis and MMP-1 are known to be downregulated and upregulated, respectively (Varani *et al.*, 2000). Results from this study provide evidence for the photobiomodulatory effects of 660 nm sequentially pulsed LED treatment.

We have previously developed a tissue-engineering approach for the production of a biological HRS from cultured human cells (Laplante *et al.*, 2001). In this study, we took advantage of this model for our *in vitro* study. The use of this tissue-engineering method allowed the creation of three differently aged HRS, which offered the unique opportunity to test biological changes, such as type-1 collagen and MMP-1 production, after LED treatment on age-defined skin. The stability of these constructs in culture over time also permitted numerous consecutive LED treatments to be applied. Results obtained from the three HRS constructs tested demonstrated that 660 nm LED exposures did not trigger histological changes; however, LED treatment significantly amplified collagen production with a concomitant decrease in collagenase (MMP-1) production. The noticeable differences between our results and those of other studies were the depth and range in collagen production increase and MMP-1 reduction in an *in vitro* milieu capable of dermal–epidermal communication comparable with that in *in vivo* skin (Weiss *et al.*, 2005; Lee *et al.*, 2007). Interestingly, LED treatments can induce similar changes in collagen synthesis and MMP activity as those reported with retinoic acid (Fisher and Voorhees 1998; Fisher *et al.*, 1998), although the mechanisms at play may be different.

The pattern of procollagen and MMP-1 production was found to be cyclic. The observed cyclical pattern could result from the capacity of HRS to express specific endogenous cell signaling pathways, periodically turning the factory ''on'' and ''off''. This was seen in both treated and untreated specimens, possibly reflecting the natural variations in procollagen and MMP regulation. Hence, LED therapy did not seem to affect the cycle *per se* but seemed to modulate the HRS intrinsic ability to do so.

The HRS model used in this study emulates skin as a complex tissue composed of two different compartments: the epidermis made up mostly of keratinocytes and the underlying dermal matrix with fibroblasts as its major cellular

components. The limitations of this model reside in the fact that it does not contain melanocytes, Merkel cells and Langerhans cells of the epidermis, skin appendages (hair and glands), vascularization and innervation of the dermis, as well as its hypodermis counterpart. More complex models are currently under development. For example, a trilayered skin substitute consisting of an epidermis, dermis, and an adipocyte-containing hypodermis has recently been produced (Trottier *et al.*, 2008). Future experiments with more complex HRS models should allow extended investigations into LED-related mechanisms.

Profilometry quantification confirmed a clinical improvement pertaining to skin surface characteristics after 1 month of LED treatment. Over 90% of participants showed a reduction in rhytid depth and surface roughness measured quantitatively by Rz and Ra PRIMOS profilometry after 12 LED treatments. Clinical improvement in wrinkles was observed in 87% of participants, although one observer reported no significant differentiation in wrinkling scores between the treated and untreated sides. Some degree of improvement was indeed noted on the untreated side in the qualitative assessments. Although photographs were randomly presented and the observers were blinded to the details of the experiment, the fact that the LED-treated side of the face was the right side in all participants may have unblinded the study and biased observers. Given that an improvement on the untreated side was also observed in the quantitative assessments, however, suggests that the improvement was genuine. The observed improvement on the untreated side could be due, at least in part, to the fact that participants were instructed on posttreatment skin care and closely monitored by the clinical team, which might have motivated them to take better care of their skin during the trial period. There is also the possibility that, as the untreated side was not covered during treatment on the controlateral side, it benefited from a spill over- or a systemic effect of treatment. Future studies with split-face designs should randomize treatment allocation with the untreated side covered.

LED therapy seemed to be well tolerated, with no adverse events or downtime reported, likely because of the absence of thermal injury to the skin during treatment. From a clinical perspective, the nonthermal characteristics of LED treatment may yield a significant advantage over other treatment methods, given that effective improvements in the appearance of aged skin can be achieved without thermal damage induced to skin with associated adverse effects. Additional studies are, however, needed to evaluate if the clinical improvements observed in this study are maintained over time, as follow-up assessments were carried out over a relatively short period of follow-up time (4 weeks). Our results are in line with previous accounts of the effectiveness of LED therapy in photorejuvenation with other light sources in which effects were observed for up to 6 months follow-up time points (Weiss *et al.*, 2004, 2005; Bhat *et al.*, 2005; Russell *et al.*, 2005; Goldberg *et al.*, 2006; Baez and Reilly, 2007; Lee *et al.*, 2007).

The induction of collagen synthesis by nonablative rejuvenation procedures has been shown to occur largely in the papillary and upper reticular dermis, forming the so-called Grenz zone (Hardaway *et al.*, 2002; Nelson *et al.*, 2002). Our results provide support for previous research showing that light in the red spectrum, such as 660 nm, allows for light penetration and absorption in the dermis and through the entire papillary layer, enabling the stimulation of collagen production (Simpson *et al.*, 1998). The cascade of events leading to collagen production is thought to be initiated by the antenna molecule mitochondrial cytochrome *c* oxidase (Karu and Kolyakov, 2005; Hamblin and Demidova, 2006; Karu *et al.*, 2005a, b). Absorbed light converted to chemical kinetic energy would cause changes in membrane permeability, improve signaling between mitochondria, nucleus and cytosol, lead to nitric oxide formation, and increase oxidative metabolism to produce more ATP (Karu, 1989; Morimoto *et al.*, 1994; Yu *et al.*, 1997; Zhang *et al.*, 2003), ultimately leading to the normalization of cell activity, including increased collagen production and MMP regulation.

To our knowledge, these are previously unreported data on the regulation of skin collagen metabolism *in vitro* with clinical correlates using a sequentially pulsed 660 nm LED source. The HRS used in this study proved to be a good preclinical model to test the effects of such light treatments on human skin over a month, and permitted to investigate the mechanism(s) responsible for the positive changes observed in the skin of LED-treated humans. The characteristics of the participants included in this trial, the study setting, the treatment regimens tested, and the outcomes assessed are similar to those encountered in day-to-day dermatology practice. The results from this study thus support 660 nm LED as a collagen-enhancement strategy that can be used safely in a clinical setting. Yet, additional studies are needed to evaluate whether 660 nm LED effects are maintained over time. Further studies are also warranted to ascertain the cellular processes involved.

IN VITRO STUDY MATERIALS AND METHODS

Cell culture media

Keratinocytes were grown in a complete DME-HAM medium: a combination of Dulbecco–Vogt modification of Eagle's medium (DME) with Ham's F12 in a 3:1 proportion (Invitrogen, Burlington, Canada), supplemented with 5% Fetal Clone II serum (FCSII) (HyClone, Logan, UT), 10 ng ml epidermal growth factor (Austral Biologicals, San Ramon, CA), 24.3 μg ml adenin (Sigma-Aldrich, Oakville, Canada), 5 μg ml insulin (Sigma-Aldrich), 5 μg ml transferrin (Roche Diagnostics, Laval, Canada), 2×10^{-9} M 3,3′ 5′ triiodo-L-thyronin (Sigma-Aldrich), 0.4 μg ml hydrocortisone (Calbiochem, La Jolla, CA), and antibiotics 100 IU ml penicillin G (Sigma-Aldrich) and 25 μg ml gentamicin (Schering, Pointe-Claire, Canada). Fibroblasts were cultured in DME containing 10% fetal calf serum (HyClone) and antibiotics.

Cell isolation and culture

Skin specimens were collected from healthy women aged 38 (HRS38), 42 (HRS42), and 64 (HRS64) years, during reductive breast surgery (HRS38 and HRS42) or face-lift (HRS64). Procedures for cell isolation were initiated within 3 hours after surgery according to a previously published method (Germain *et al.*, 2001; Auger *et al.*,

2002). Skin specimens were washed five times with a phosphate-buffered saline supplemented with antibiotics. Specimens were then cut into 3 mm wide strips and kept overnight at 4 °C in Hepes buffer containing 500 µg ml thermolysin. The epidermis was mechanically separated from the dermis with forceps; keratinocytes were dissociated from the epidermis through incubation of the epidermal fragments under agitation at 37°C for 30 minutes, with 0.05% trypsin-0.1% EDTA in PBS. After trypsin inactivation (addition of culture medium containing 10% serum and centrifugation), keratinocytes were expanded in the presence of irradiated 3T3 fibroblasts in T75 flasks (BD Biosciences, Mississauga, Canada) and subsequently frozen until further use. Fibroblasts were dissociated from the remaining dermis fragments after incubation in a collagenase H solution at 37°C under agitation. After centrifugation, the fibroblasts were also plated in T75 flasks for expansion and subsequently frozen until further use.

Production of tissue-engineered HRS

The cells isolated from the healthy women aged 38, 42, and 64 years were used to reconstruct HRS38, HRS42, and HRS64, respectively. HRS were produced as previously described (Michel *et al*. 1999). Briefly, fibroblasts (F38, F42, or F64) were cultivated in a fibroblast culture medium containing 50 µg ml sodium ascorbate (Sigma-Aldrich) for 4 weeks until cell sheets were formed. After peeling the fibroblast sheets from the bottom of the dishes, two sheets were superimposed, for a total of two sheets per HRS, and cultured for 1 week. After dermal equivalent maturation, keratinocytes (250,000 cells per cm^2, between cellular passages 2 and 3) were seeded on reconstructed stroma and cultured for 7 days in a keratinocyte complete medium (containing 50 µg ml sodium ascorbate) under submerged conditions. The HRS were then brought to the air–liquid interface and cultivated in complete DME-HAM with 5% serum and 50 µg ml sodium ascorbate, without EGF, for an additional 4 weeks. The culture medium was changed three times per week. Each experimental condition was tested in triplicate on the three HRS tested (HRS38, HRS42, and HRS64). All plastic ware for tissue culture was procured from BD Biosciences.

LED and sham light treatments

Samples of the HRS replicates were exposed to the LED or sham light source under a laminar flow hood. HRS were treated 11 times (T1 to T11) over a 1-month period, treatments were performed three times a week for 4 consecutive weeks, with only two treatments performed in the fourth week. Cultures were then incubated at 37°C (8% CO_2). Supernatants were collected before each treatment and after the last treatment, and stored at −20°C until assessed for type I procollagen and MMP-1.

The LED technique involved the application of a 660-nm wavelength delivered in a sequential pulsing mode at a power density of 50 mW cm for a total fluence of 4 J cm, for a duration of 160 seconds (2m40 s) (LumiPhase-R, OPUSMED Inc. Montreal, Canada). The pulsing patterns and time on and time off sequences were as follows: Pulse width (time on) 500 µsec, pulse interval (time off) 150 µsec, four pulses per pulse train, and a pulse train interval of 1,550 µsec. The non-treated HRS samples were exposed to a sham light for 160 seconds with a total fluence of 0 J cm.

During this study, a lot of care was taken to maintain a working distance of 2.5 cm (± 1 mm) away from the target surface during LED therapy, as power density/light intensity—a key variable for optimal photoinduction—is greatly influenced by the distance between the light source and the surface of the skin (Hart and Cameron, 2005). Measurements of the intensity (mW) of the LED light source emitting at 660 nm (110 mA CW) were taken with a ph100-si (Gentec-eo, Quebec, Canada) at every centimeter, up to a 10-cm distance away from the light source. This was important to ensure that the proper amount of photons was delivered to reach the cellular activation (induction) threshold in the skin.

Type I collagen and MMP-1 determination

Human type I collagen was measured in cell culture supernatants of the selected time period with the Protype I collagen C-peptide enzyme immunoassay kit purchased from Takara Mirus Bio (Madison, WI), according to the manufacturer's instructions. MMP-1 levels were also measured using MMP-1 biotrak activity assay systems according to the manufacturer's instructions (Amersham Biosciences, Baie D'Urfe, Canada).

Data analysis

As an indication of effect size to measure the direction and magnitude of the treatment effect for each time point, Cohen's *d* was used. Cohen's *d* was computed as follows: *d* is the difference in group means divided by the pooled s.d. A standardized effect size of 0.2 is considered small, 0.5 is considered medium, and 0.8 is considered large (Cohen, 1988).

Histological analysis

After the last treatment, biopsies of untreated and LED-treated reconstructed skin were fixed for at least 24 hours in a Bouin solution (ACP, St Leonard, Canada) and embedded in paraffin. Five-µm-thick cross-sections were stained with Masson's trichrome. Photographs were taken at the ×40 objective with a digital camera (CoolSnap RS Photometrics, Roper Scientific, Munich, Germany).

Indirect immunofluorescence microscopy

At the end of the treatment series, samples of the untreated and LED-treated reconstructed skin were embedded and frozen in OCT compound (Somagen, Edmonton, Canada). Four-µm-thick cross-sections were fixed in cold acetone and further incubated with mouse monoclonal anti-human type I collagen antibody (Chemicon, Temecula, CA). The secondary antibodies (Chemicon) used were rhodamine-conjugated goat anti-mouse IgG-IgM and goat anti-rabbit IgG. Nuclei were stained blue with Hoechst 33258 (Sigma-Aldrich).

IN VIVO STUDY MATERIALS AND METHODS

Participant selection

Forty healthy patients with aged/photoaged skin (37 women and 3 men) with a mean age of 44.9 (33–62) years were recruited from the Dr. Daniel Barolet Clinic in Montreal, Canada from September 2002 to December 2002 and tested between January 03 and April 03. Inclusion criteria included patients with skin type I to III according to the FCS (Fitzpatrick, 1988). At study entry, 15% of patients were skin type I, 45% were skin type II, and 40% were skin type III. A total of 48% were deemed to present with mild, 38% with moderate, and 10% with a severe degree of wrinkles, according to the FSC for degree of wrinkling (rhytids).

Exclusion criteria comprised patients taking cortisone (prednisone), anticoagulant therapy, or any drug known to increase photosensitivity. In addition, during the 12 months preceding the study, patients were required not to have used isotretinoin (Accutane) or applied topical steroids to the site to be treated. Moreover, a previous laser or topical medication at the to-be-treated site was not permitted. Patients gave written, informed consent to participate in this trial in compliance with the US Code of Federal Regulations dealing with the conduct of clinical studies (21CFR including parts 50 and 56 with regard to informed consent and IRB regulations). The study was conducted according to Good Clinical Practice Guidelines and the principles of the Declaration of Helsinki, and was approved by the Institutional Review Board Services (Div. 1373737 Toronto, Canada). The trial was registered with ClinicalTrials.Gov (ClinicalTrials.gov Identifier: NCT00818246). The study flow chart is presented in Figure 5.

Study design

This was a split-face single-blinded study to assess the efficacy of LED treatment on overall skin appearance (rhytids depth and texture—surface roughness) of the aged/photoaged periorbital area. This study design allowed for within-participant assessments of clinical effects. Assignment: The right periorbital area was designated to be the experimental side, and the left periorbital was used as control (sham light). Blinding: The observers who performed the clinical qualitative assessments on the basis of digital photographs were blinded to the treatment regimen (LED-treated or untreated/control side) and to the timing of the photographs (pre- or posttreatment).

Study procedure

Participants were treated three times weekly for 4 consecutive weeks (12 treatments) with the 660 nm-pulsed LED device on the experimental periorbital area. LED treatments were administered using the same parameters as those for the *in vitro* study (see *In vitro* Study Materials and Methods). To maximize LED photoinduction, a topical moisturizer without active ingredients was applied daily, as dry skin is known to enhance skin surface reflectivity (Friedman *et al.*, 2002). To support photobiochemical reactions in the triggering of gene-expression-enhanced collagen metabolism during LED exposure, skin temperature should be kept normal, that is, physiological (Halper *et al.*, 2005). Therefore, monitoring papillary dermis temperature with a needle probe (type-T thermocouple from Omega, Montreal, Canada) during LED treatment was carried out. The control side was exposed to a sham light for 160 seconds with a total fluence of 0 J cm. No cooling method was used after exposure. To avoid hiding periorbital skin, a well-circumscribed external eyelid protector (Oculoplastik, Montreal, Canada) was worn to protect the retina from direct illumination. Before returning home, participants were instructed on posttreatment skin care, which included applying a plain moisturizer on both sides of the face, sun avoidance, and the use of a sunscreen (SPF 30).

Primary outcome measures

A topographical quantitative assessment was carried out for each study participant using PRIMOS 3D surface topography (GFM, Teltow, Germany) profilometry performing phase shift rapid *in vivo* measurements of skin from the experimental and control periorbital areas before treatment and 4 weeks after treatment. A PRIMOS readings (PRIMOS 4 Software, GFM, Teltow, Germany) star analysis was carried out, from a phase shift photograph, a 1.5 cm-diameter circular portion of the skin on the lateral cantus area was cut into 12 equal segments, allowing depth calculation of fine surface lines (peak and valley analysis) in that area and quantification of skin surface roughness. The Ra value was calculated from general surface roughness characteristics, pore size and skin texture. The Rz value obtained for each participant was

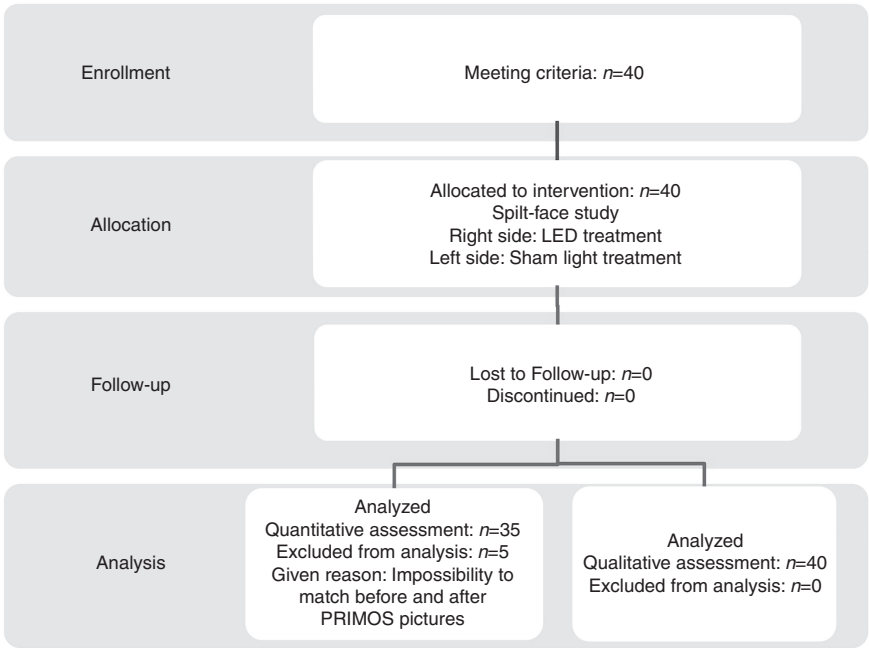

Figure 5. Clinical study flow chart.

estimated from average peak and valley measurement data to quantify rhytid depth and severity. Pre- and posttreatment surface topography measurements were taken to precisely quantify clinical improvements.

Secondary outcome measures

A clinical qualitative assessment was carried out by three blinded medical observers through the evaluation of digital photographs (Canon Dual Flash E2, Mississauga, Canada) of the experimental and control periorbital areas taken pre-treatment and 4 weeks posttreatment for each participant. Each photograph was taken maintaining identical ambient lighting, pose, and camera angles. To avoid bias in clinical appraisal, sets of photographs for the treated and untreated sides of the face were randomly presented to the observers who were blinded to the details of the experiment. The photographs were analyzed for clinical improvement using the FCS subtype scale for degree of wrinkling (rhytids). Their assessment was rated on a five-point scale and scored as follows: 0 = none, 1 = mild, 2 = moderate, 3 = good, 4 = excellent. Adverse effects were monitored over the entire course of the study.

Data analysis

Sample sizes and power calculations were generated according to the primary outcome measures of the study. To have a 98% chance of detecting as significant (at the two-sided 5% level) a 10% difference between the treated and untreated/control sides in the Ra and Rz posttreatment improvement, with an assumed s.d. of 10, 33 participants were required. To account for an 80% per protocol completion rate, the planned number of patients to be enrolled was 40.

The primary outcome variables were the percent improvement posttreatment for the Ra and Rz values measured 4 weeks posttreatment. The primary outcome analysis was conducted on results from 35 participants. The data from five participants were removed from the quantitative assessment analysis because of the fact that it was not possible to match the before and after PRIMOS data digital color-coded photographs. The secondary clinical outcome variable was the medical observers' combined gain in the FCS score for degree of wrinkling 4 weeks after treatment. Secondary outcome analysis was conducted on the results of the total sample of participants ($n = 40$). For the primary and secondary outcome variables, an analysis of covariance was used to assess statistical differences between the LED-treated and untreated sides, taking into account age as the covariate. Main effects and two-way interactions were incorporated into the statistical model. Tukey's HSD test was used to assess pairwise comparisons. Cronbach's α was calculated to assess internal consistency between the observers' assessments. *P*-values were considered significant at $P \leqslant 0.05$.

CONFLICT OF INTEREST

Intellectual Property disclosure related to the LED pulsing code by the first author.

ACKNOWLEDGMENTS

We thank the following people for their indispensable contribution to this study: Isabelle Lussier Ph.D. from MedStrategis for her assistance (article & biostatistical analysis), Geneviève Chaput, Mathieu Auclair, Diane Lamalice, François Barolet, Lyne Jodoin, Chémir Mamode, Jean Dubé, Dominique Gignac, and Mariane Moisan.

REFERENCES

Auger FA, Rémy-Zolghadri M, Grenier G, Germain L (2002) A truly new approach for tissue engineering: The LOEX self-assembly technique. In: *Stem cell transplantation and tissue engineering*, (Haverich A, Graf H, eds). Springer-Verlag: Berlin, 73–88

Baez F, Reilly LR (2007) The use of light-emitting diode therapy in the treatment of photoaged skin. *J Cosmet Dermatol* 6:189–94

Barolet D, Boucher A, Bjerring P (2005) *In vivo* human dermal collagen production following LED-based therapy: the importance of treatment parameters. *Lasers Surg Med* 17:76. (abstract)

Barolet D (2008) Light-emitting diodes (LEDs) in dermatology. *Semin Cutan Med Surg* 27:227–38

Bhat J, Birch J, Whitehurst C, Lanigan SW (2005) A single-blinded randomised controlled study to determine the efficacy of Omnilux Revive facial treatment in skin rejuvenation. *Lasers Med Sci* 20:6–10

Cohen J (1988) *Statistical power analysis for the behavioral sciences*. 2nd ed, Lawrence Earlbaum Associates: Hillsdale, NJ

Fisher GJ, Kang S, Varani J, Bata-Csorgo Z, Wan Y, Datta S *et al.* (2002) Mechanisms of photoaging and chronological skin aging. *Arch Dermatol* 138:1462–70

Fisher GJ, Talwar HS, Lin J, Lin P, McPhillips F, Wang Z *et al.* (1998) Retinoic acid inhibits induction of c-Jun protein by ultraviolet radiation that occurs subsequent to activation of mitogen-activated protein kinase pathways in human skin *in vivo*. *J Clin Invest* 101:1432–40

Fisher GJ, Voorhees JJ (1998) Molecular mechanisms of photoaging and its prevention by retinoic acid: ultraviolet irradiation induces MAP kinase signal transduction cascades that induce Ap-1-regulated matrix metalloproteinases that degrade human skin *in vivo*. *J Investig Dermatol Symp Proc* 3:61–8

Fisher GJ, Varani J, Voorhees JJ (2008) Looking older: fibroblast collapse and therapeutic implications. *Arch Dermatol* 144:666–72

Fitzpatrick TB (1988) The validity and practicality of sun-reactive skin types I through VI. *Arch Dermatol* 124:869–71

Fligiel SEG, Varani J, Datta SH, Kang S, Fisher GJ, Voorhees JJ (2003) Collagen degradation in aged/photoaged skin *in vivo* and after exposure to MMP-1 *in vitro*. *J Invest Dermatol* 120:842–8

Friedman PM, Skover GR, Payonk G, Kauvar AN, Geronemus RG (2002) 3D *in-vivo* optical skin imaging for topographical quantitative assessment of non-ablative laser technology. *Dermatol Surg* 28: 199–204

Germain L, Moulin V, Berthod F, Lopez C.A, Goulet F, Auger FA (2001) Multiple applications of tissue-engineered human skin. In: *Cultured human keratinocytes and tissue engineered skin substitutes*. (Horch RE, Munster AM, Achauer BM eds). Georg Thieme Verlag: Stuttgart, Germany, 91–8

Goldberg DJ, Amin S, Russell BA, Phelps R, Kellett N, Reilly LA (2006) Combined 633-nm and 830-nm led treatment of photoaging skin. *J Drugs Dermatol* 5:748–53

Halper J, Griffin A, Hu W, Jung C, Zhang J, Pan H *et al.* (2005) *In vitro* culture decreases the expression of TGF(beta), Hsp47 and type I procollagen and increases the expression of CTGF in avian tendon explants. *J Musculoskelet Neuronal Interact* 5:53–63

Hamblin MR, Demidova TN (2006) Mechanisms of low level light therapy. In: *Mechanisms for Low-Light Therapy* (Michael R. Hamblin, MR, Waynant RW, Anders J eds). Proc of SPIE V 6140 1–12

Hardaway CA, Ross EV, Barnette DJ, Paithankar DY (2002) Nonablative cutaneous remodeling with a 1.45 microm mid-infrared diode laser: phase I. *J Cosmet Laser Ther* 4:3–8

Hart G, Cameron R (2005) The importance of irradiance and area in neonatal phototherapy. *Arch Dis Child Fetal Neonatal Ed* 90:F437–40

Huang PJ, Huang YC, Su MF, Yang TY, Huang JR, Jiang CP (2007) *In vitro* observations on the influence of copper peptide aids for the LED photoirradiation of fibroblast collagen synthesis. *Photomed Laser Surg* 25:183–90

Kang S, Fisher GJ, Voorhees JJ (2001) Photoaging: pathogenesis, prevention, and treatment. *Clin Geriatr Med* 17:643–59

Karu T (1989) Photobiology of low-power laser effects. *Health Phys* 56:691–704

Karu TI, Kolyakov SF (2005) Exact action spectra for cellular responses relevant to phototherapy. *Photomed Laser Surg* 23:355–61

Karu TI, Pyatibrat LV, Afanasyeva NI (2005a) Cellular effects of low power laser therapy can be mediated by nitric oxide. *Lasers Surg Med* 36: 307–14

Karu TI, Pyatibrat LV, Kolyakov SF, Afanasyeva NI (2005b) Absorption measurements of a cell monolayer relevant to phototherapy: reduction of cytochrome c oxidase under near IR radiation. *J Photochem Photobiol B* 81:98–106

Laplante AF, Germain L, Auger FA, Moulin V (2001) Mechanisms of wound reepithelialization: hints from a tissue-engineered reconstructed skin to long-standing questions. *FASEB J* 15:2377–89

Lee SY, Park KH, Choi JW, Kwon JK, Lee DR, Shin MS *et al.* (2007) A prospective, randomized, placebo-controlled, double-blinded, and split-face clinical study on LED phototherapy for skin rejuvenation: clinical, profilometric, histologic, ultrastructural, and biochemical evaluations and comparison of three different treatment settings. *J Photochem Photobiol B* 27:51–67

McDaniel DH, Weiss RA, Geronemus R, Ginn L, Newman J (2002) Light–tissue interactions I: Photothermolysis versus photomodulation laboratory findings. *Lasers Surg Med* 14:25 (abstract)

Meireles GC, Santos JN, Chagas PO, Moura AP, Pinheiro AL (2008a) A comparative study of the effects of laser photobiomodulation on the healing of third-degree burns: a histological study in rats. *Photomed Laser Surg* 26:159–66

Meireles GC, Santos JN, Chagas PO, Moura AP, Pinheiro AL (2008b) Effectiveness of laser photobiomodulation at 660 or 780 nanometers on the repair of third-degree burns in diabetic rats. *Photomed Laser Surg* 26:47–54

Michel M, L'Heureux N, Pouliot R, Xu W, Auger FA, Germain L (1999) Characterization of a new tissue-engineered human skin equivalent with hair. In Vitro *Cell Dev Biol Anim* 35:318–26

Morimoto Y, Arai T, Kikuchi M, Nakajima S, Nakamura H (1994) Effect of low intensity Argon laser irradiation on mitochondria respiration. *Lasers Surg Med* 15:191–9

Nelson JS, Majaron B, Kelly KM (2002) What is nonablative photorejuvenation of human skin? *Semin Cutan Med Surg* 21:238–50

Russell BA, Kellett N, Reilly LR (2005) A study to determine the efficacy of combination LED light therapy (633 and 830 nm) in facial skin rejuvenation. *J Cosmet Laser Ther* 7:196–200

Simpson CR, Kohl M, Essenpreis M, Cope M (1998) Near-infrared optical properties of ex vivo human skin and subcutaneous tissues measured using the Monte Carlo inversion technique. *Phys Med Biol* 43:2465–78

Trottier V, Marceau-Fortier G, Germain L, Vincent C, Fradette J (2008) IFATS collection: using human adipose-derived stem/stromal cells for the production of new skin substitutes. *Stem Cells* 26:2713–23

Varani J, Schuger L, Dame MK, Leonard C, Fligiel SE, Kang S *et al.* (2004) Reduced fibroblast interaction with intact collagen as a mechanism for depressed collagen synthesis in photodamaged skin. *J Invest Dermatol* 122:1471–9

Varani J, Warner RL, Gharaee-Kermani M, Phan SH, Kang S, Chung JH *et al.* (2000) Vitamin A antagonizes decreased cell growth and elevated collagen-degrading matrix metalloproteinases and stimulates collagen accumulation in naturally aged human skin. *J Invest Dermatol* 114:480–6

Weiss RA, McDaniel DH, Geronemus R, Weiss MA (2005) Clinical trial of a novel non-thermal LED array for reversal of photoaging: clinical, histologic, and surface profilometric results. *Lasers Surg Med* 36:85–91

Weiss RA, Weiss MA, Geronemus RG, McDaniel DH (2004) A novel non-thermal non-ablative full panel LED photomodulation device for reversal of photoaging: digital microscopic and clinical results in various skin types. *J Drugs Dermatol* 3:605–10

Yu W, Naim JO, McGowan M, Ippolito K, Lanzafame RJ (1997) Photomodulation of oxidative metabolism and electron chain enzymes in rat liver mitochondria. *Photochem Photobiol* 66:866–71

Zhang Y, Song S, Fong CC, Tsang CH, Yang Z, Yang M (2003) cDNA microarray analysis of gene expression profiles in human fibroblast cells irradiated with red light. *J Invest Dermatol* 120:849–57